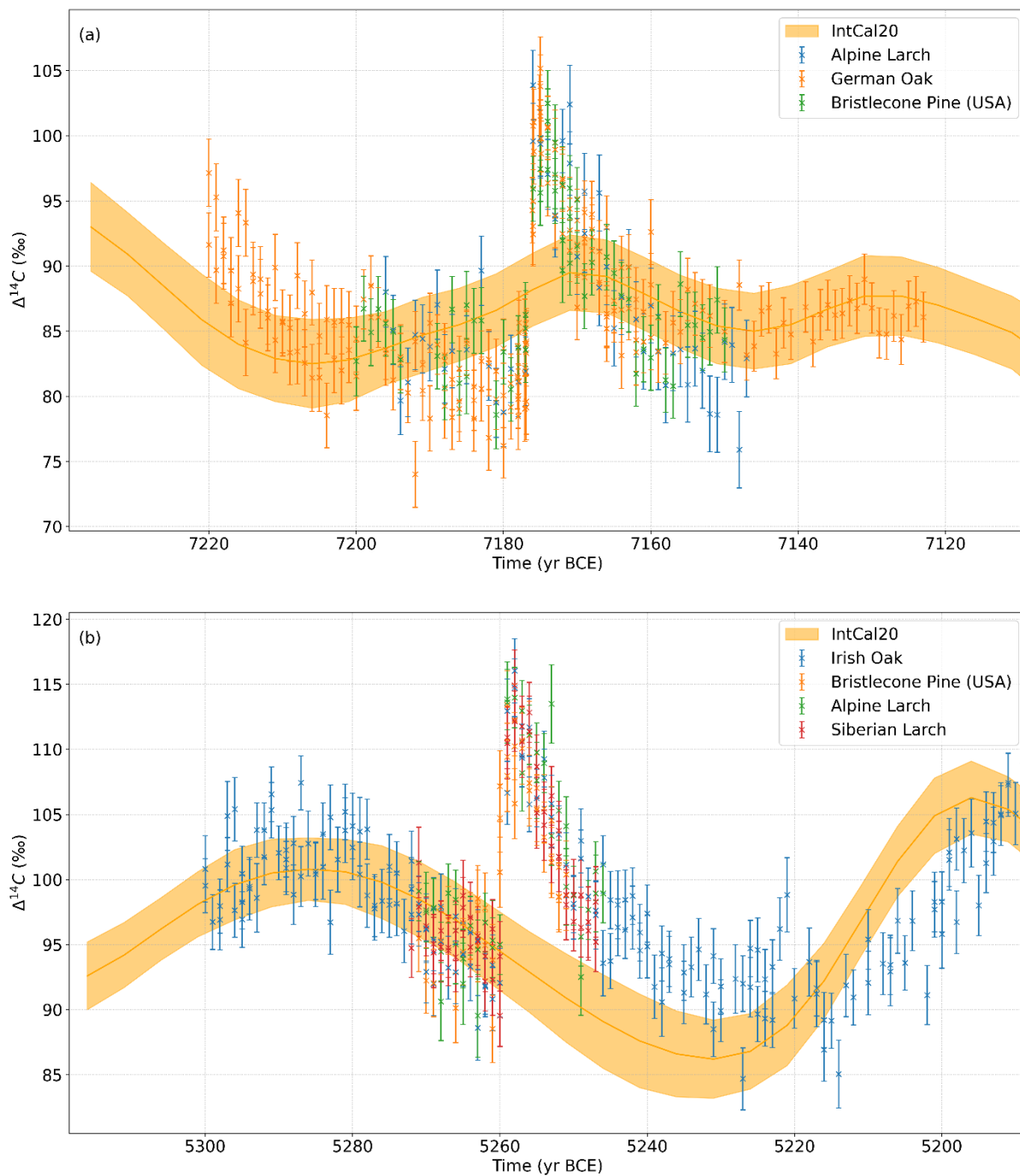
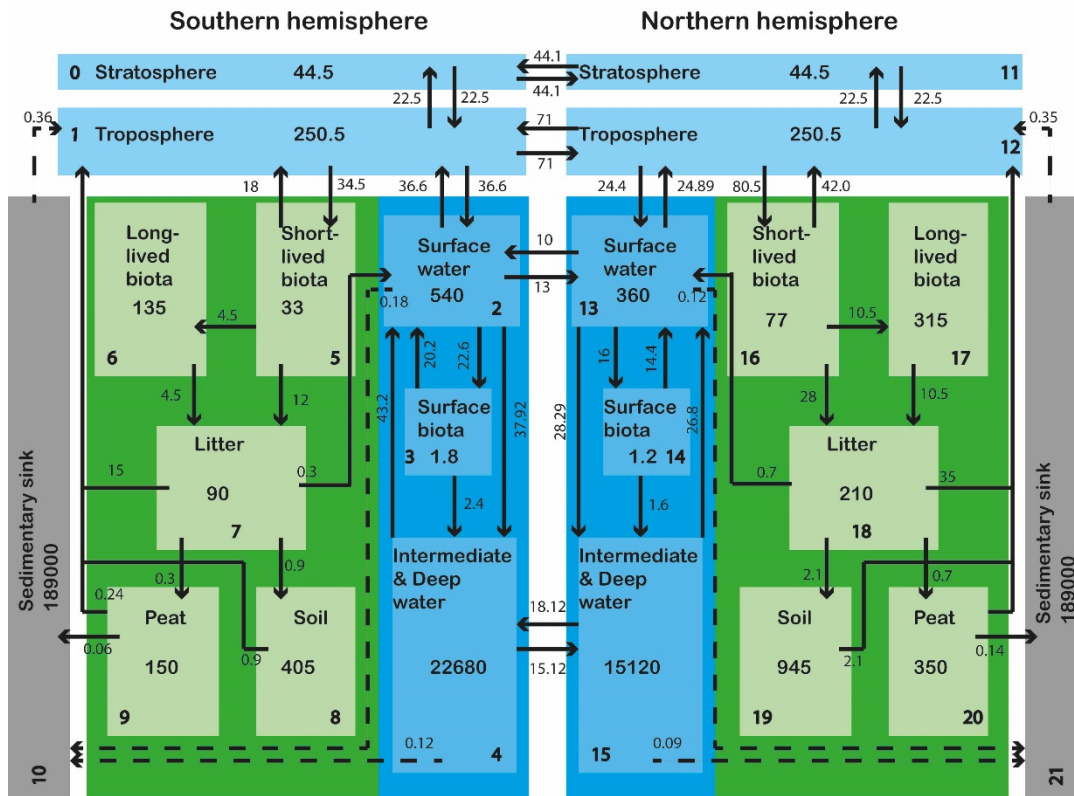


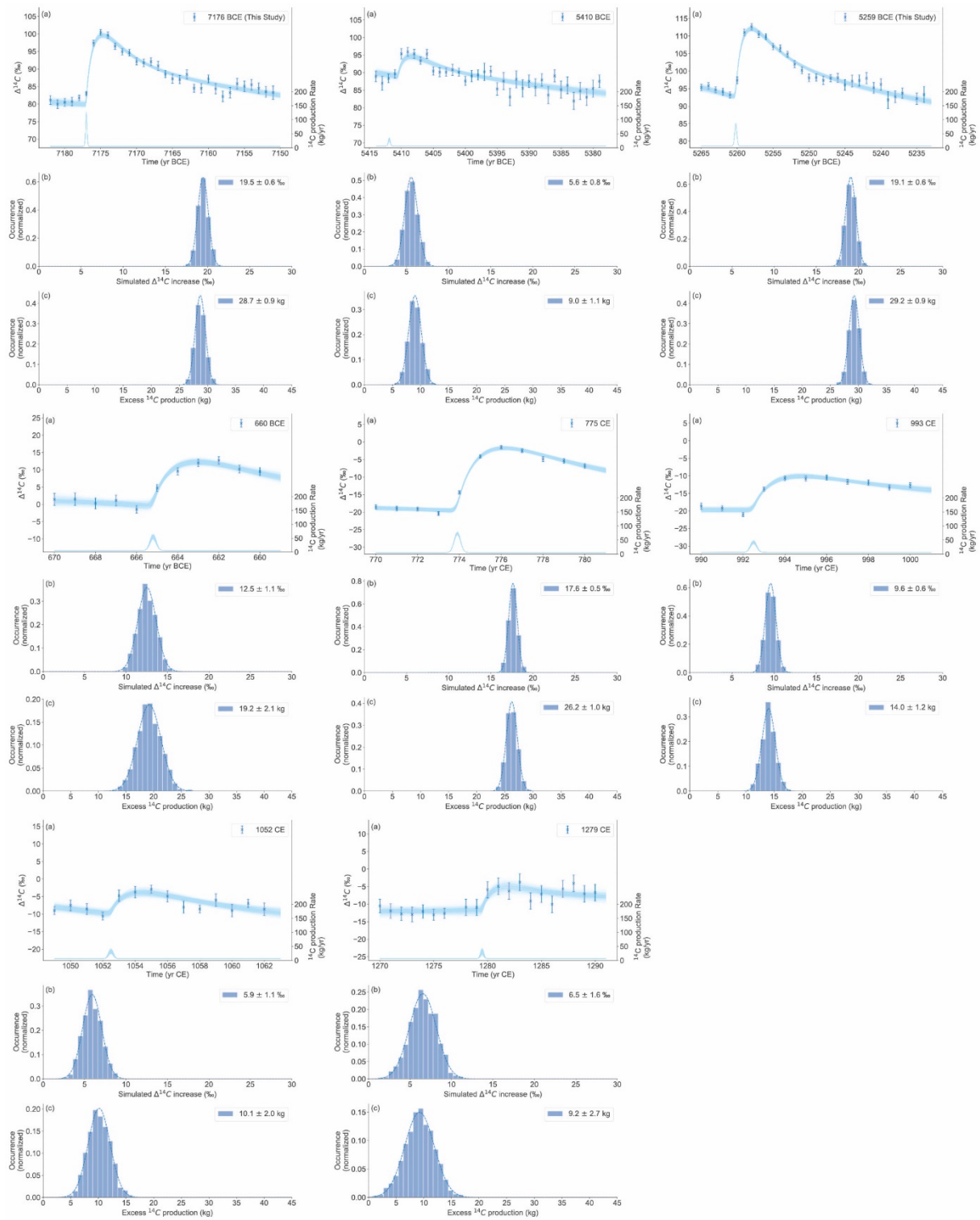
Supplementary figures



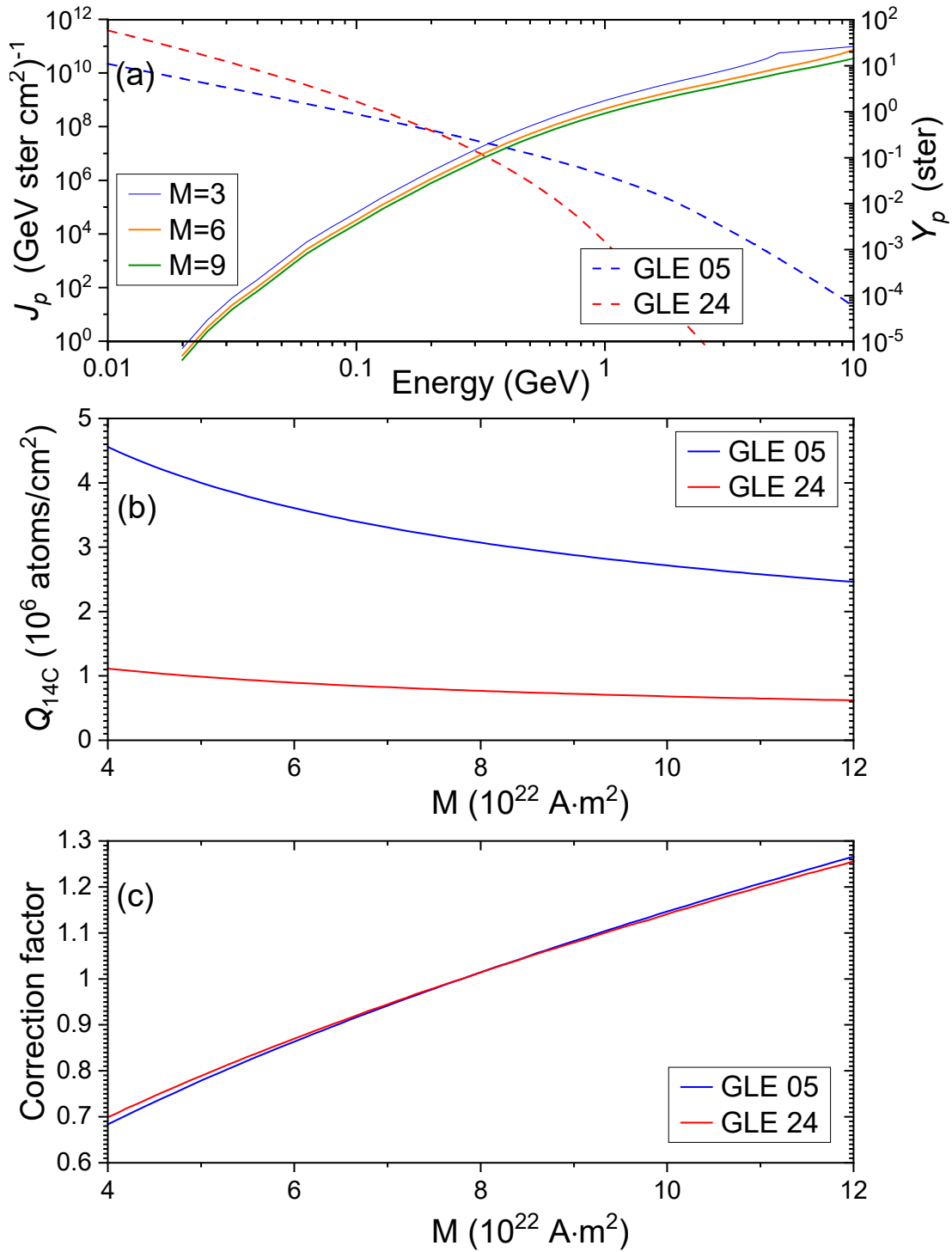
Supplementary Fig. 1 All Measurement results of the 2 new events. ^{14}C measurements with 1- σ errors reported as $\Delta^{14}\text{C}$ of the two newly found events (7176 BCE (a), 5259 BCE (b)) in all different trees compared to the IntCal20 calibration curve¹ (orange band). The Irish Oak was independently repeated by two different labs (ETH-Zurich, Bristol).



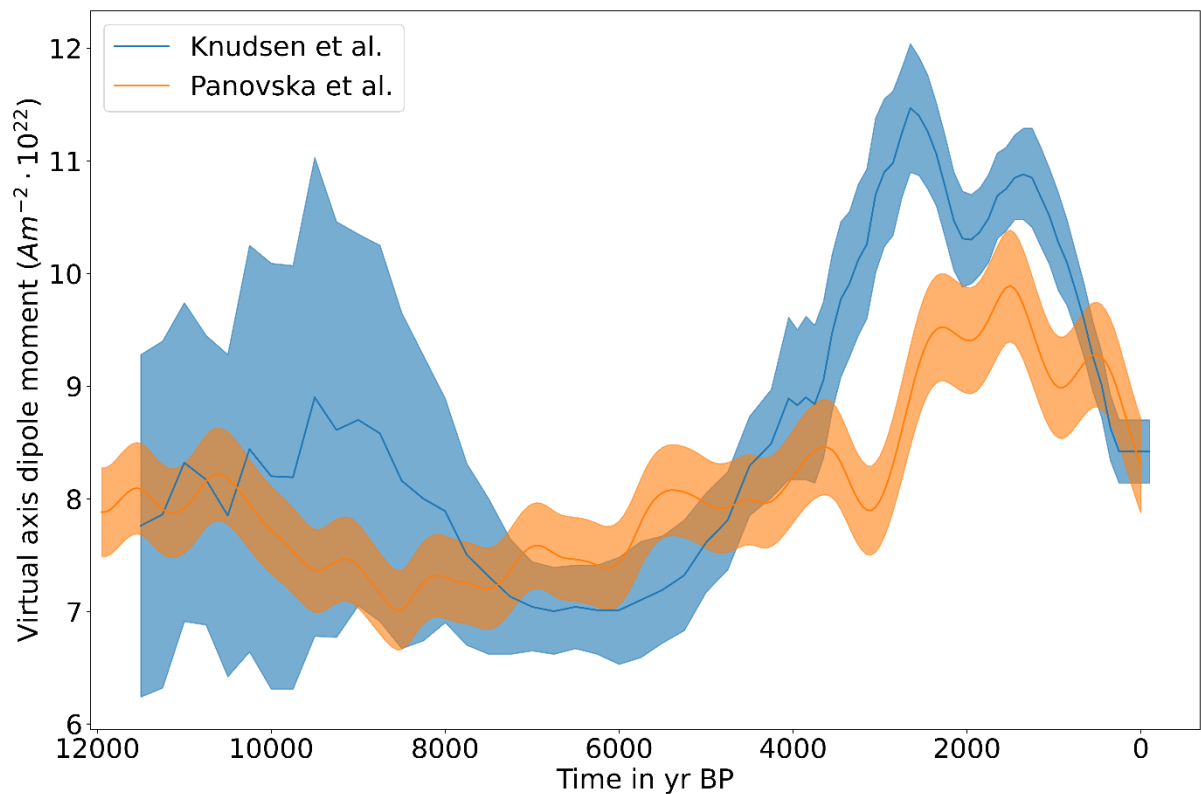
Supplementary Fig. 2 Carbon box model used to reconstruct ^{14}C production. The carbon fluxes between boxes and their carbon contents are given in Gt/yr and Gt.



Supplementary Fig. 3 Evaluation of all known ^{14}C events. (a) Mean data of known ^{14}C events with $1\text{-}\sigma$ errors and result of 1000 Simulations. The fitted Gaussian shaped production spikes for all simulations are also shown. (b) Distribution of the simulated $\Delta^{14}\text{C}$ increases (blue bars) with a Gaussian fit (dashed line). (c) Distribution of excess ^{14}C production (blue bars) with Gaussian fit (dashed line). Data Sources: 5410 BCE: Miyake et al.², 660 BCE: Sakurai et al.³, 775 CE and 993 CE: Büntgen et al.⁴, 1052 CE and 1279 CE: Brehm et al.⁵.



Supplementary Fig. 4 Production of ^{14}C by SEP events for different values of VADM: (a) Global yield functions (Y_p , right-hand-side axis) of ^{14}C by protons for three values of VADM (3x, 6x and 9x 10^{22} A m 2 as blue, orange and green solid lines, respectively); as well as spectral omnidirectional fluences ($J(E)$, left-hand-side axis) of SEPs for two bounding cases, the softest and hardest-spectrum known events of 23-Feb-1956 (GLE 05, blue dashed line) and 04-Aug-1972 (GLE 24, red dashed line). (b) Calculated globally-averaged ^{14}C production $Q_{14\text{C}}$ during the two SEP events as a function of the geomagnetic field VADM. (c) Correction factor $Q(M_o)/Q(M)$ of the ^{14}C production at the VADM value of M to that for a modern geomagnetic field ($M_o=7.8 \cdot 10^{22}$ A m 2).



Supplementary Fig. 5 Comparison of two geomagnetic field reconstructions. Two geomagnetic field reconstructions by Knudsen et al.⁶ (blue) and Panovska et al.⁷ (orange) over the last 12000 years including 1- σ uncertainty ranges.

Supplementary References

- 1 Reimer, P. J. *et al.* The IntCal20 Northern Hemisphere Radiocarbon Age Calibration Curve (0–55 cal kBP). *Radiocarbon* **62**, 725-757, doi:10.1017/RDC.2020.41 (2020).
- 2 Miyake, F. *et al.* A Single-Year Cosmic Ray Event at 5410 BCE Registered in 14C of Tree Rings. *Geophys Res Lett* **48**, e2021GL093419, doi:10.1029/2021GL093419 (2021).
- 3 Sakurai, H. *et al.* Prolonged production of 14C during the ~660 BCE solar proton event from Japanese tree rings. *Scientific Reports* **10**, 660, doi:10.1038/s41598-019-57273-2 (2020).
- 4 Büntgen, U. *et al.* Tree rings reveal globally coherent signature of cosmogenic radiocarbon events in 774 and 993 CE. *Nature Communications* **9**, doi:10.1038/s41467-018-06036-0 (2018).
- 5 Brehm, N. *et al.* Eleven-year solar cycles over the last millennium revealed by radiocarbon in tree rings. *Nature Geoscience* **14**, 10-15, doi:10.1038/s41561-020-00674-0 (2021).
- 6 Knudsen, M. F. *et al.* Variations in the geomagnetic dipole moment during the Holocene and the past 50 kyr. *Earth and Planetary Science Letters* **272**, 319-329, doi:10.1016/j.epsl.2008.04.048 (2008).
- 7 Panovska, S., Constable, C. G. & Korte, M. Extending Global Continuous Geomagnetic Field Reconstructions on Timescales Beyond Human Civilization. *Geochemistry, Geophysics, Geosystems* **19**, 4757-4772, doi:10.1029/2018GC007966 (2018).